AIAA JOURNAL
Vol. 34, No. 4, April 1996

Flow Control over a Maneuvering Delta Wing at High Angles of Attack

Sandra M. Klute,* Othon K. Rediniotis,† and Demetri P. Telionis‡
Virginia Polytechnic Institute and State University, Blacksburg, Virginia 24061-0219

The possibility of delaying vortex breakdown to higher angles of attack by employing control surfaces is studied experimentally. The effect of an apex flap is tested for fixed and dynamically pitching delta wings. Flow visualization, surface pressure measurements, and laser-Doppler velocimetry are employed to map out pressure, velocity, and vorticity fields. It is found that a drooping apex flap can delay vortex breakdown by an angle of 8 deg beyond the steady flow breakdown angle of attack. The apex flap effect is equally pronounced in dynamic maneuvers.

Introduction and Background

AT high angles of attack, vortex breakdown dominates the aerodynamics of swept lifting surfaces. The occurrence of this phenomenon is accompanied by drastic changes in the pressure distribution, which in turn strongly affect the attitude of an aircraft. It is desirable to control the onset of vortex breakdown, delay it, or induce it at will. This is particularly needed for controlled flight at high angles of attack.

Various methods have been tested to control vortex breakdown at high angles of attack. Most of the significant work in this area until 1990 was reviewed by Lee and Ho.[1] Recently, attention has been paid to the use of blowing and suction to achieve localized control of the leading-edge vortices. Experiments have been performed by Wood and Roberts,[2] and Wood et al.[3] in which steady blowing has been utilized to control vortices emanating along curved leading edges. Gad-el-Hak and Ho[4] employed sinusoidal perturbations of a high frequency. For the case of blowing along the leading edge, a delay in the vortex breakdown position has been reported by Wiseer et al.[5] Magness et al.[6,7] and later Gu et al.[8] employed cyclic blowing and suction to delay vortex breakdown and stabilize the flow over delta wings at high angles of attack.

At moderate angles of attack, flaps have been employed to influence forces and moments over delta wings. Lamar[9] experimented with a single trailing-edge aileron, tip mounted onto a cropped delta wing. This successfully generated a constant rolling moment. In addition, a vortex flow roll-control device was designed to develop flow asymmetries through modification of the planform geometry. Results indicate a potentially useful device in which the effect of increasing the angle of a raked-tip leading edge is to produce an almost linear increase in rolling moment. However, these tests were confined to angles of attack less than 30 deg. Rao and Campbell[10] discuss several effects of vortical flow generators, including leading-edge vortex flaps that can operate either on the lower or upper surface of a delta wing. It is clear that these devices have potential over various different flight regimes. A detailed description of contributions in this area is included in Ref. 11.

In the present paper we explore the effectiveness of a deployable surface, an apex flap, to control the flow over a delta wing. The emphasis here is on larger angles of attack, and therefore the aim is to control, delay, or induce vortex breakdown. Schaeffler et al. have reported on the effectiveness of cavity flaps on vortex breakdown.[12] Results on a few other devices were reported by the present authors in Ref. 13. Other authors[14,15] also reported on the effectiveness of devices such as leading-edge flaps to control vortex breakdown in dynamic wing motions but considered angles of attack not higher than 35 deg. Here we very briefly discuss the results with such devices and concentrate on the most effective device, the apex flap, carrying the investigation up to an angle of attack of 50 deg. Moreover, and for the first time, we explore the effectiveness of such a device on a dynamically developing vortical field. This is the case of a delta wing during a pitching up motion.

Facilities and Instrumentation

Tests were conducted in two different facilities, a 10×12 in. water tunnel and a wind tunnel with a test section of 20×20 in. Three-component laser-Doppler velocimetry (LDV) was employed in the water tunnel, and surface pressure data were obtained in the wind tunnel. The LDV system is a TSI system operating in backscatter with a 35-mW helium-neon laser. Mirrors, traversing mechanisms, and lead screws operated by stepping motors facilitate displacement of the measuring volume. Measuring grids normal to the oncoming stream can thus be automatically traversed. The measuring volume can be positioned on a grid point with an accuracy of $\pm$ 0.1 mm through the use of two LVDTs that are incorporated in a position feedback loop. Two components of the velocity are measured simultaneously from each side of the tunnel, and the three-dimensional field is later constructed.

Experiments were conducted with fixed as well as with dynamically pitching models. The motion chosen was a swift pitch up about the apex, followed by a slow return to the initial angle of attack. Data were obtained in the wind tunnel at 100 discrete instances during the pitch up and were ensemble averaged over 200 realizations of the motion. Only seven realizations were averaged in the water tunnel after tests indicated that the flow was highly repeatable. In both tunnels, a trigger was provided from the driving mechanism. In addition, an encoder recorded the angle of attack at each of the sampling points to monitor the instantaneous position of the model. The ramplike motion involved a constant angular velocity ω. The dimensionless pitch rate $\omega c/2U_\infty$ was 0.06, where c and U_∞ are the chordlength and the freestream velocity, respectively.

The entire operation was controlled by two serially communicating laboratory computers that were programmed to operate the pitching mechanism and the stepping motors, collect the information on the instantaneous angle of attack, perform the LDV or pressure data acquisition, reduce and ensemble average the data, and transfer them to a mainframe IBM 3090 for calculations and plotting.

Two delta wing models with 75-deg sweep angle were employed with sizes designed to achieve approximately the same blockage ratio in both facilities. The models were mounted on dynamic struts that could position them at a fixed angle of attack or, alternatively, carry them into pitch-up motions with arbitrarily described schedules. Both models had a thickness-to-chord ratio of 0.042 and a bevel angle of 45 deg on their windward side. They were geometrically similar to the models employed earlierly by the present group.[16–18]

Presented as Paper 93-3494 at the AIAA 11th Applied Aerodynamics Conference, Monterey, CA, Aug. 9–11, 1993; received April 28, 1994; revision received April 4, 1995; accepted for publication April 18, 1995.

*Graduate Student, Department of Engineering Science and Mechanics.
†Assistant Professor, Department of Engineering Science and Mechanics.
‡Professor, Department of Engineering Science and Mechanics. Associate Fellow AIAA.

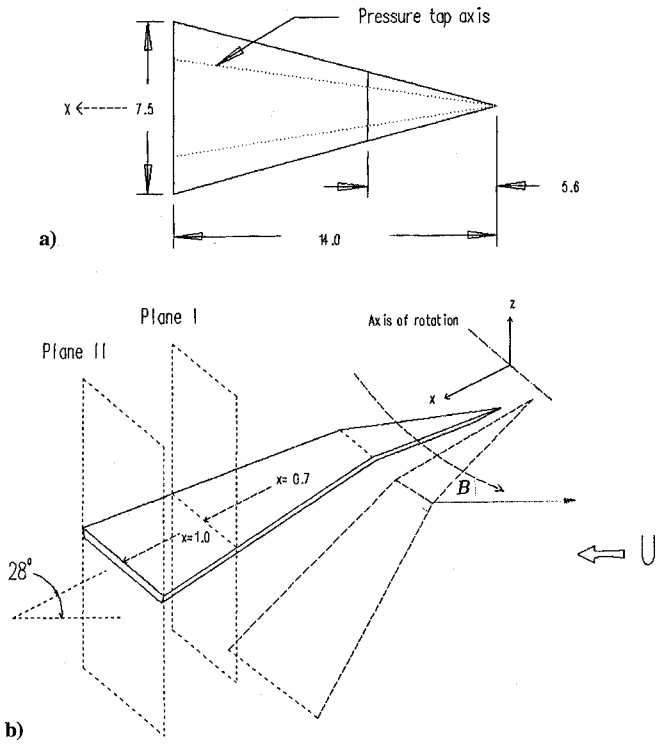

Fig. 1 Delta wing model with a drooping apex flap: a) planform (dimensions in inches) and b) the pitch-up motion and the planes of measurement.

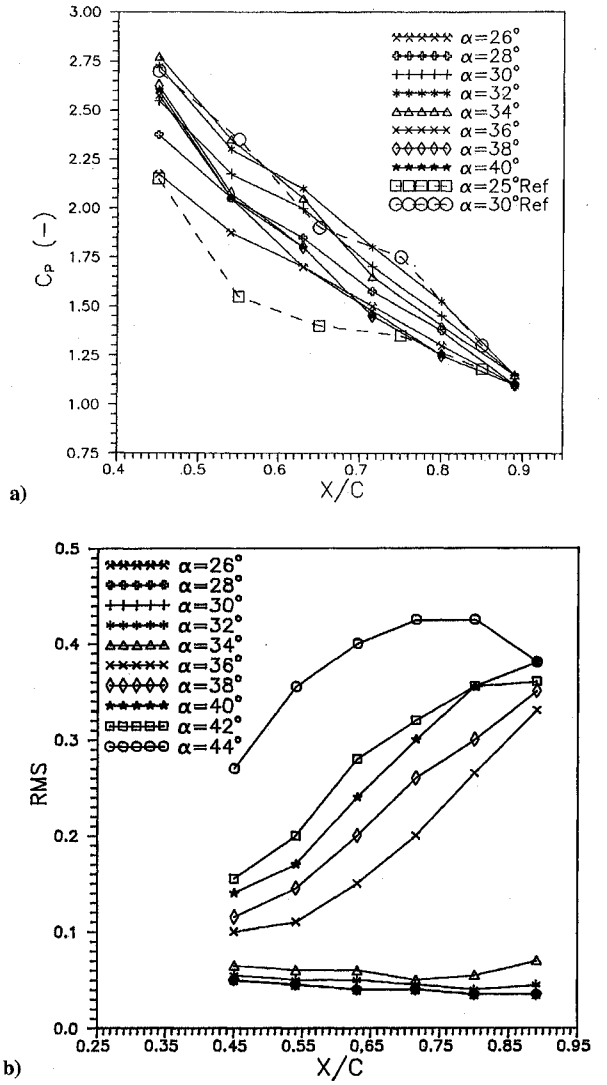

Fig. 2 Steady flow over the basic configuration: a) mean pressure and b) rms of pressure.

The model employed in the wind tunnel is shown in Fig. 1a. The front portion of both models was hinged and could be drooped as shown in Fig. 1b. The angle of droop is denoted by the symbol B. The upper surface of the model was equipped with pressure taps connected to a miniature PSI pressure scanner along an axis approximately beneath the vortex axis. The location of this axis was determined by earlier studies[16–18] of the present group to be 6.4 deg inboard of the leading edge. The model employed in the water tunnel was geometrically similar but was not equipped with pressure transducers. Both models could be tested in their basic shape, as well as with a drooping apex flap.

LDV data were obtained along two fixed vertical planes, denoted as planes I and II as shown in Fig. 1b. At the initial angle of attack, $\alpha = 28$ deg, these two planes intersect the wing section at chordwise locations of 0.7 and 1, respectively. The second plane corresponds to the trailing edge at $\alpha = 28$ deg. During pitch up about an axis passing through the undeflected apex, plane I cuts the wing planform at locations corresponding to even higher chordwise locations.

An extensive uncertainty analysis for the present experimental rig was carried out. The reader can find details in Ref. 19. The laser-Doppler velocimeter is sensitive to the velocity component given by $V = f_D(\lambda/2\sin\kappa)$, where f_D is the Doppler frequency, λ is the wavelength of the laser light, and κ is half the beam crossing angle. Using $w_f = 0.01 f_D$ as a worst case for the uncertainty on the frequency, and $w_k = 0.25\kappa$ for the beam alignment uncertainty, a velocity uncertainty of $w_v = 0.027U_\infty$ (20:1) is calculated. In the wind tunnel the combined inaccuracy of the pressure transducers, transducer calibration, amplifiers, and data acquisition board is estimated as $\pm 0.0347 C_p$ at $U_\infty = 12$ m/s (20:1).

Results and Discussion

The flow over a delta wing is dominated by two leading-edge vortices. Such vortices are characterized by high axial velocity and vorticity, but these features may suddenly change if the vortices break down.[1,11] The axial velocity then goes to zero and subsequently reverses direction while vorticity diminishes significantly. Vortex breakdown creeps up from downstream and at a certain angle of attack reaches the trailing edge of the wing. This condition is often referred to as the onset of breakdown. With further increases of the angle of attack, breakdown moves up over the wing and towards the apex, until the vortex is broken down along the entire chord. The wing is then stalled. The development of breakdown is monitored in our experiments via pressure and LDV measurements.

Steady flow experiments were conducted first in the wind tunnel. Mean and rms values of pressure over an unmodified model at various angles of attack are displayed in Fig. 2. Data are presented in terms of the nondimensionalized distance from the apex of the model along the axis of the wing. In this figure we also display selected data from Ref. 20 for comparison. In general, results compare well, both at the apex and trailing edge. Some differences occur as the half-chord region is approached, which may be because the model employed by these authors had a double-beveled edge.

As the angle of attack increases, the static pressure decreases monotonically, until breakdown enters the domain over the wing. The location of vortex breakdown is characterized by a local slight increase of the streamwise pressure distribution. This increase appears as a crossover of the pressure distribution over the curve corresponding to the smaller angle of attack. For example, in Fig. 2a, the pressure line of $\alpha = 34$ deg crosses that of $\alpha = 32$ deg at $x/c = 0.59$. Flow visualization was conducted, and the results confirmed this to be an accurate streamwise breakdown position for $\alpha = 34$ deg. Further increase in the angle of attack involves a further lowering of the pressure over the entire region of measurement. A purely phenomenological observation made in every test is that the curvature of the streamwise pressure distribution changes sign at the breakdown angle of attack.

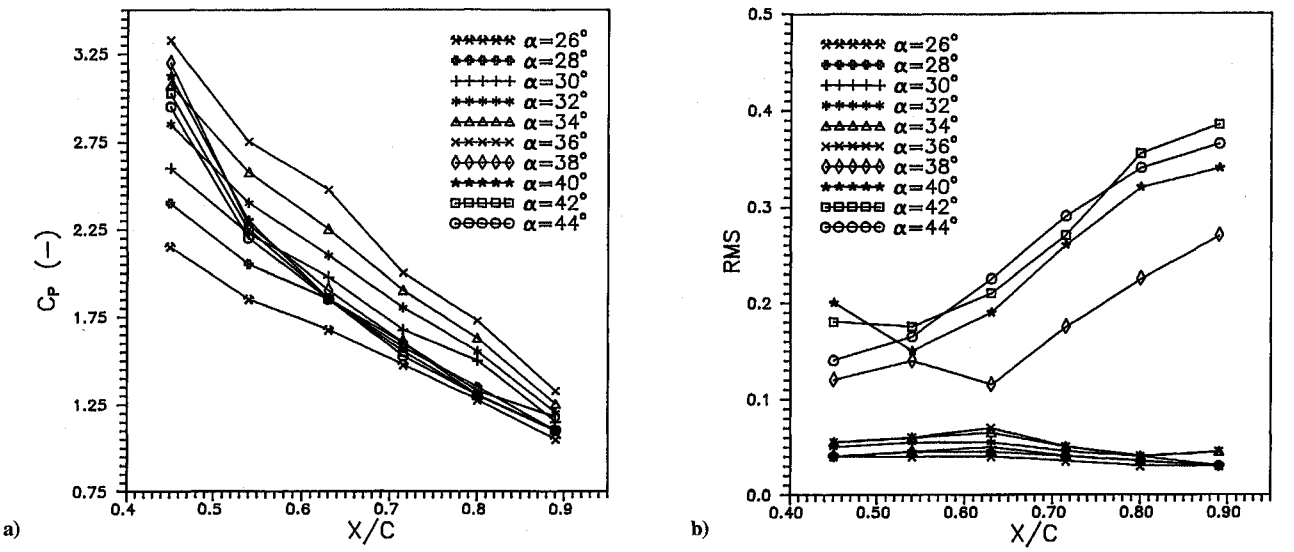

Fig. 3 Pressure distribution on suction surface, with drooping apex flap at B = 8 deg: a) mean pressure and b) rms.

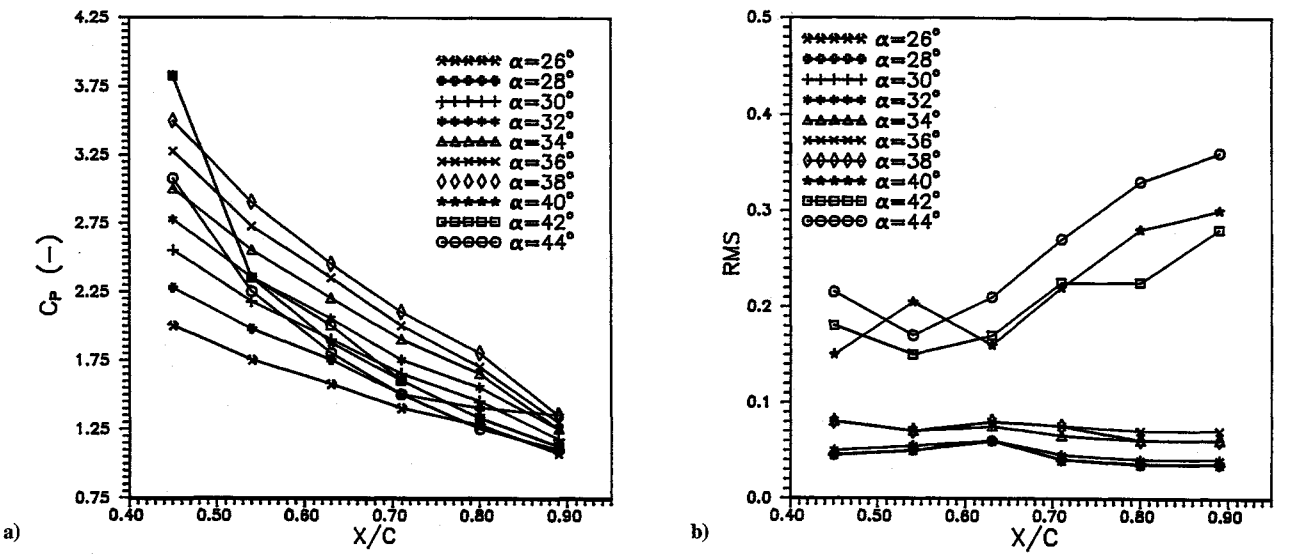

Fig. 4 Pressure distribution on suction surface with drooping apex at B = 12 deg: a) mean pressure and b) rms.

Breakdown can also be detected by a drastic increase in the rms level. Figure 2b shows that at $\alpha = 34$ deg a slight increase in the rms occurs at the pressure port nearest the trailing edge. A drastic increase in the rms follows for $\alpha = 36$ deg, with values as high as 0.32 at the trailing edge. It is interesting to note that the loss in pressure magnitude always slightly precedes the increase in its rms.

A number of control surfaces in the form of fences or flaps attached on the windward or leeward side of the wing were tested. However, their effectiveness in controlling the vortices at high angles of attack was surpassed by the apex flap. Data on the performance of such devices were included in Ref. 13. Here we confine our discussion to the results obtained with an apex flap.

Results obtained with the apex flap are presented in Figs. 3–5 for drooping apex flap angles of $B = 8$, 12, and 18 deg, respectively. A considerable delay of breakdown is now observed. For $B = 8$ deg, Fig. 3a shows clearly that at $\alpha = 36$ deg the pressure over the entire wing is still decreasing beyond the level corresponding to smaller angles of attack. It is not until $\alpha = 38$ deg that the pressure suddenly rises. The rms measurements in Fig. 3b confirm this delay in breakdown. Data are next presented in Fig. 4 for $B = 12$ deg. A further delay in breakdown is observed. Pressure remains low for $\alpha = 38$ deg and suddenly rises for $\alpha = 40$ deg. Between $\alpha = 38$ and 40 deg, the breakdown position has moved from the trailing edge to a position forward of $x/c = 0.45$.

The apex flap was next positioned at $B = 18$ deg. The rms pressure distribution presented in Fig. 5b shows low values until $\alpha = 42$ deg. Before breakdown, in both Figs. 4b and 5b, rms values seem to be higher at the first pressure port and then decrease towards the trailing edge. This could result from turbulence created by the vortex bending around the corner of the apex flap and main wing. In Fig. 5a the pressure for $\alpha = 42$ deg crosses that of $\alpha = 40$ deg at $x/c = 0.45$. This is almost the maximum delay in vortex breakdown observed for any deflection angle of the apex flap. Tests were conducted at seven deflection angles between 6 and 18 deg. These results are not shown here due to lack of space but indicated that the optimal deflection angle, i.e., the maximum breakdown delay corresponds to $B = 15$ deg.

Next, we considered the corresponding pressure and velocity field during dynamic pitch-up motions. Pressures taken on the unmodified model at a reduced pitch-up rate of 0.06 display a characteristic delay in breakdown.[4,17,18,21–24] Well-behaved, coherent vortices exist up to an angle of attack $\alpha = 45$ deg (Fig. 6). Breakdown appears for $\alpha = 46.5$ deg and has already moved upstream of the trailing edge, up to $x/c = 0.66$. Making use of the encouraging results

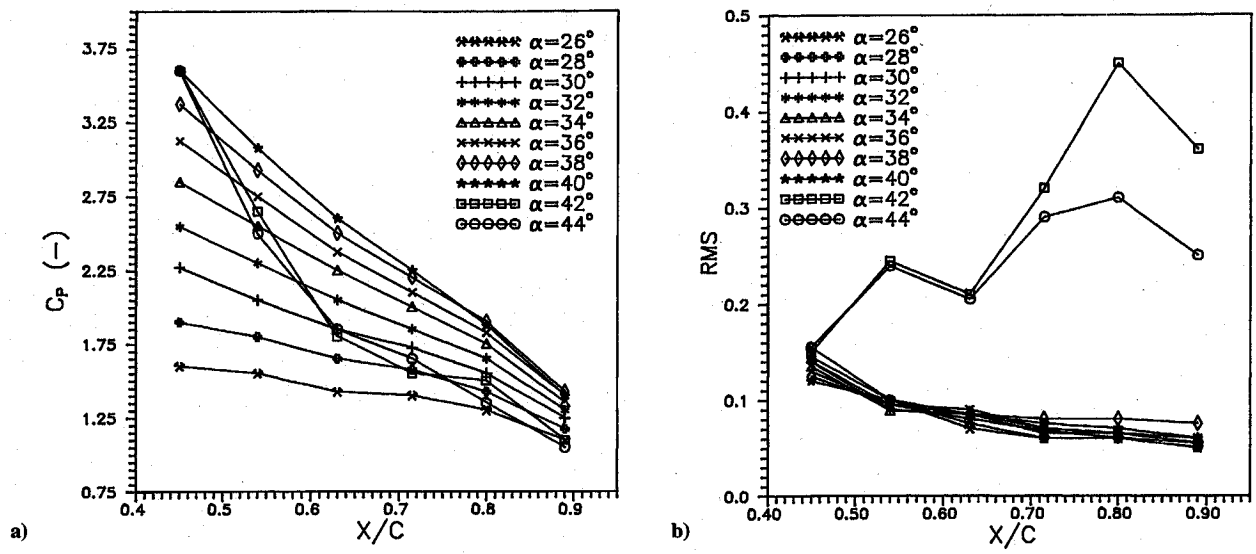

Fig. 5 Pressure distribution on suction surface with drooping apex at B = 18 deg: a) mean pressure and b) rms.

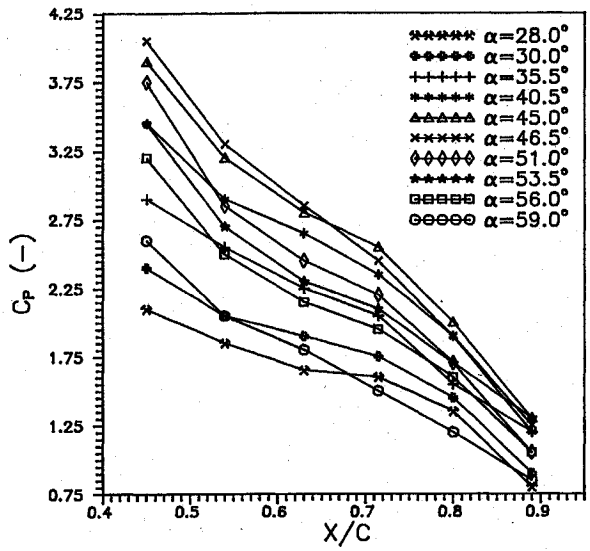

Fig. 6 Unsteady axial pressure distribution during pitch up with B = 0 deg.

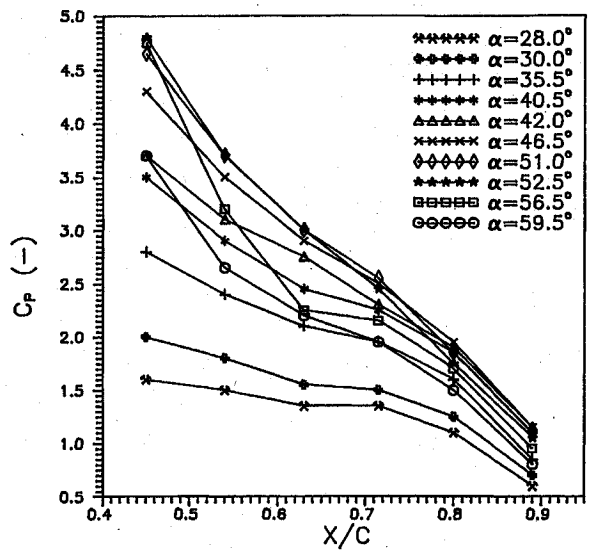

Fig. 7 Unsteady axial pressure distribution during pitch up with B = 15 deg.

obtained with the apex flap in our steady work, the flap was deployed at B = 15 deg during a pitch-up maneuver. Results are plotted in Fig. 7 for comparison against those in Fig. 6. Here breakdown has been delayed to 52.5 deg.

To further verify these findings, three-component LDV data were obtained in the water tunnel and are presented in Figs. 8–11. In Fig. 8, velocity vectors in the crossflow plane are plotted along with axial velocity contours over the wing for the unmodified wing and the wing with the apex flap deployed.[§] Note that here the measuring plane is fixed and corresponds to $x/c = 0.70$ at the initial angle of attack of α = 28 deg. The wing actually maneuvers through this fixed plane, so that for α = 50.5 deg the plane of measurement corresponds to $x/c = 0.96$. The position of this plane is marked as plane I in Fig. 1. Data along a second fixed plane, plane II (Fig. 1), were also obtained and will be presented in Fig. 9.

As the wing retreats, a larger domain becomes available for measurement on its upper surface, and thus the area populated by data appears growing in each of the frames of the figures that follow. The lowest line of data defines the intersection of the measuring plane and the wing surface. Moreover, the projection of the trailing edge to the plane of data is also marked by a horizontal line. Figure 8a presents data with an unmodified wing, whereas Fig. 8b contains data obtained with an apex flap deployed at an angle B = 15 deg. Breakdown characterized by an axial flow stagnation region develops over the plain wing and spreads from the inboard region towards the center of the core. This behavior may be a little misleading, because our axial component is along the freestream direction and not along the instantaneous axis of the vortex. However, the behavior of the velocity component along the vortex axis is not much different as pointed out by Rediniotis et al.[16]

The zero velocity region approaches the core from the wing and therefore in violation of the axisymmetric nature of the flow. This feature was also observed and reported earlier for steady flow by Kegelman and Roos.[25] For the unmodified wing, breakdown along the plane of measurement is initiated at α = 38 deg and dominates the flowfield at α = 42.5 deg.[¶] On the other hand, the core of the vortex over the wing with a deployed apex flap contains much higher values of velocity and for much larger angles of attack. In Fig. 8b, it appears that breakdown does not develop until α = 50.5 deg. In fact, these data indicate that the axial velocity increases in the core of the vortex even up to α = 46.5 deg.

[§]In the CD-ROM version of this paper, Figs. 8 and 9 present in color instantaneous frames at α = 28, 34, 38, 42.5, 46.5, and 50.5 deg. The files of the actual experimental data are also included.

[¶]These are shown only in the CD-ROM version of the paper.

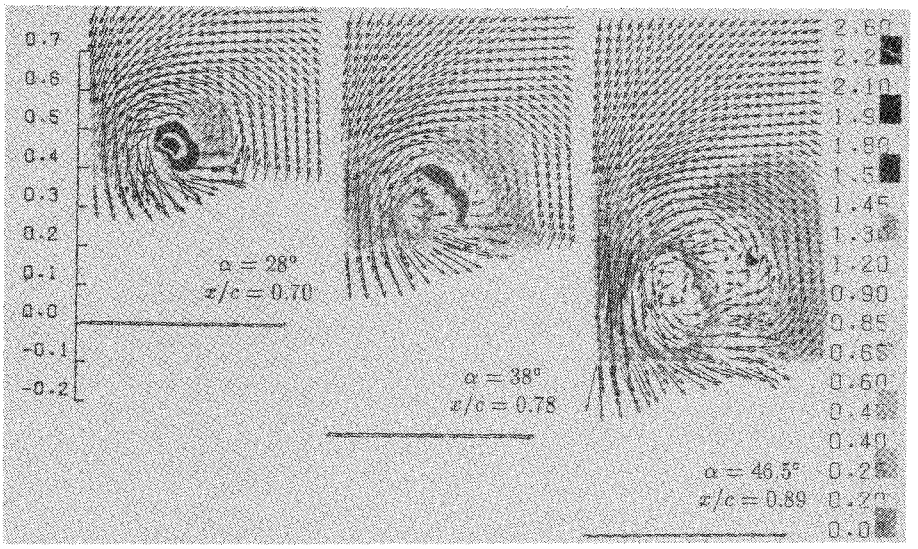

Fig. 8a Axial velocity contours and crossflow velocity vectors over an unmodified delta wing (plane I) performing a pitch-up motion at a rate of $\omega c/2U_\infty = 0.06$.

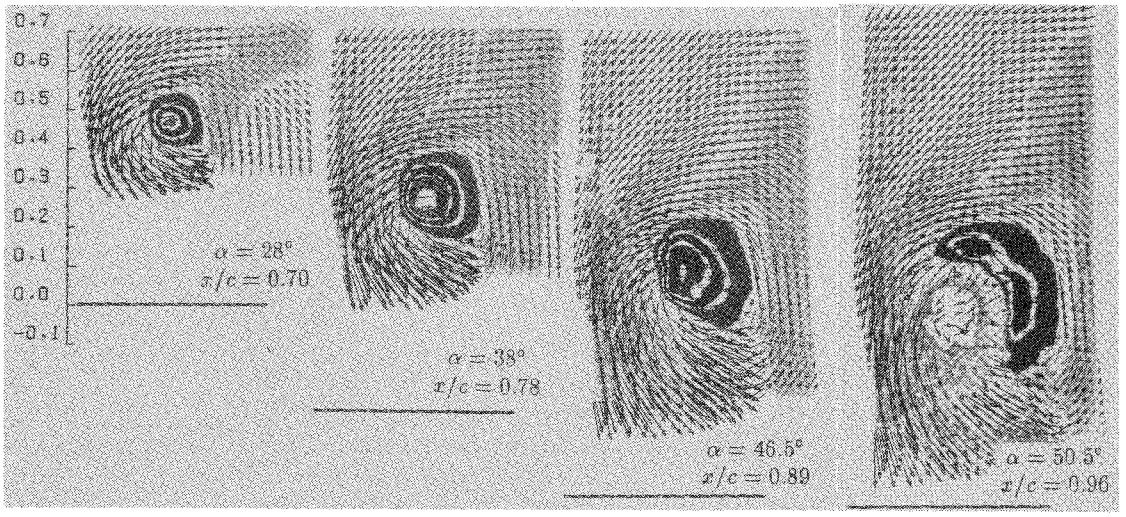

Fig. 8b Axial velocity contours and crossflow velocity vectors over a delta wing (plane II) with an apex flap deployed at $B = 15$ deg performing a pitch-up motion.

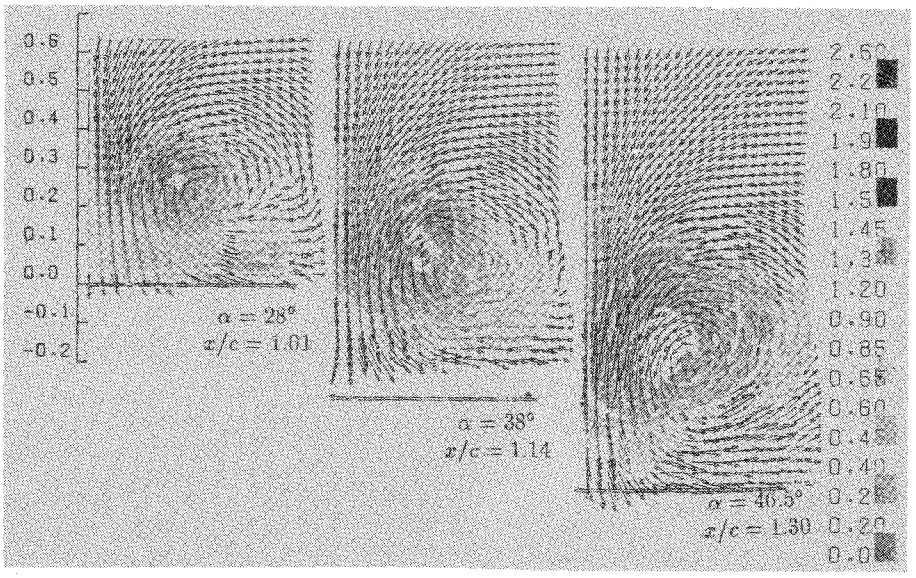

Fig. 9a Axial velocity contours and crossflow velocity vectors in the wake of an unmodified delta (plane II) wing performing a pitch-up motion.

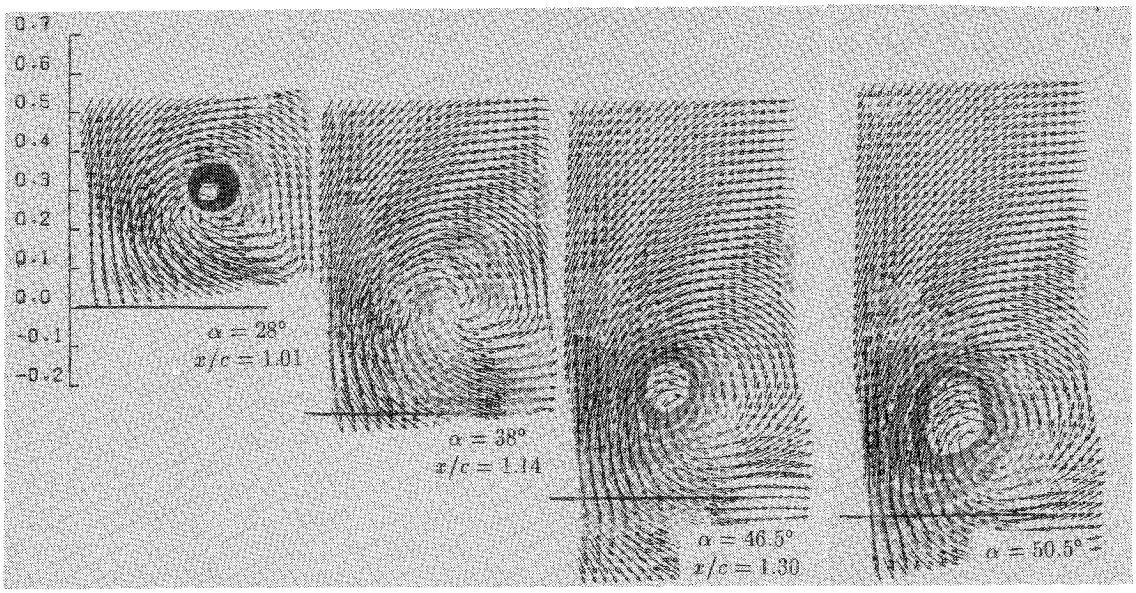

Fig. 9b Axial velocity contours and crossflow velocity vectors in the wake of a delta wing (plane II) with an apex flap deployed at B = 15 deg performing a pitch-up motion.

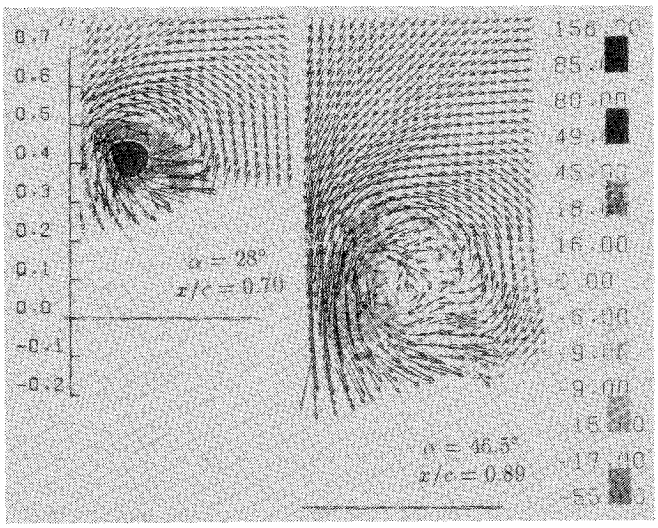

Fig. 10a Vorticity contours and crossflow velocity vectors (plane I) over an unmodified delta wing performing a pitch-up motion.

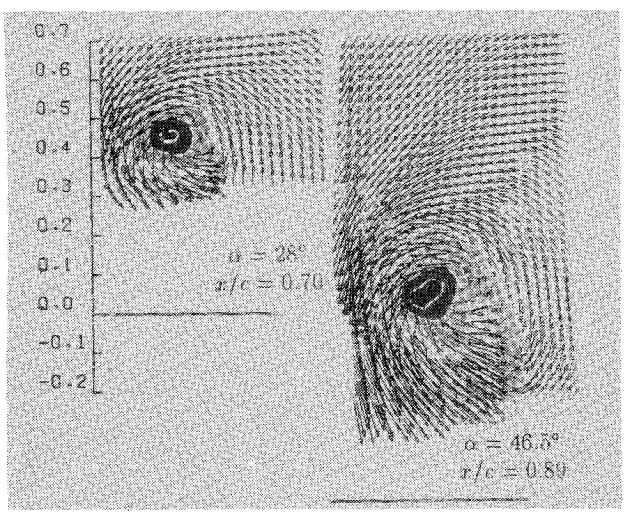

Fig. 10b Vorticity contours and crossflow velocity vectors over a delta wing (plane I) with an apex flap deployed at B = 15 deg performing a pitch-up motion.

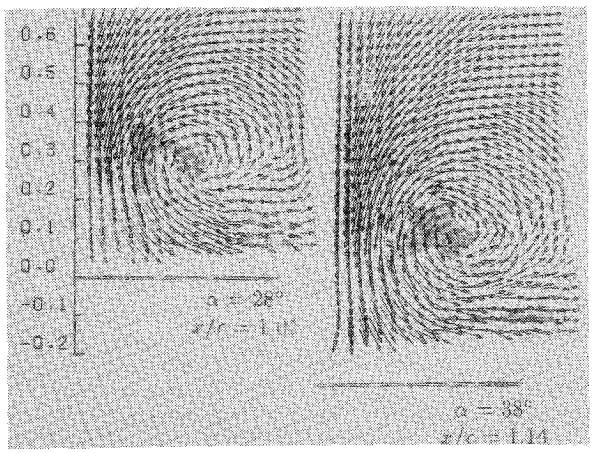

Fig. 11a Vorticity contours and crossflow velocity vectors in the wake (plane II) of an unmodified delta wing performing a pitch-up motion.

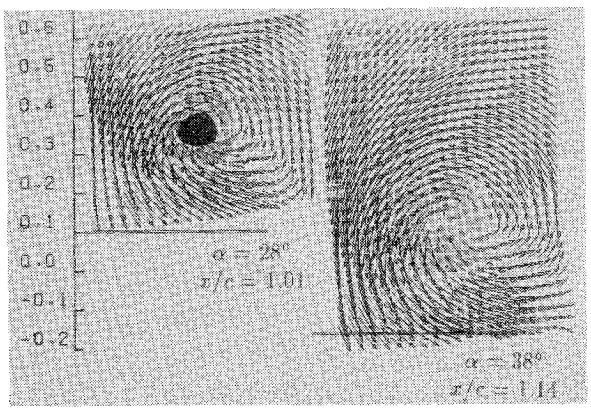

Fig. 11b Vorticity contours and crossflow velocity vectors in the wake (plane II) of a delta wing with an apex flap deployed at B = 15 deg performing a pitch-up motion.

In Fig. 9 we display similar results obtained along plane II (Fig. 1). The flow over the unmodified wing is totally broken down, and yet some coherence and axial velocities larger than U_∞ can be observed over the droop-nosed wing, even up to $\alpha = 38$ deg.‖

Vorticity contours are presented for the two stations I and II (Fig. 1) over the droop-nosed wing in Figs. 10 and 11, respectively.

‖These are also shown only in the CD-ROM version of the paper.

Again, it appears that the modified wing retains vorticity coiled in a nearly axisymmetric pattern up to $\alpha = 46.5$ deg at the $x/c = 0.70$ station. Opposite sense of vorticity, representing secondary vortices, can be observed near the wing surface. A comparison of the vorticity contours in Fig. 10b with the axial velocity contours of Fig. 8b also indicates that vorticity retains a coherent distribution, consistent with the ordered circumferential distribution of the velocity. In other words, vorticity contours nearly coincide with the circumferential streamline loops as conjectured by the circumferential velocity components. Vortex sheets are therefore nearly coincident with stream tubes. On the other hand, the axial velocity distribution is skewed. The low-speed region is approaching from the inboard region. A significant delay in loss of vorticity is also observed in Fig. 11b where we present the results obtained along plane II.

Conclusions

Breakdown is characterized by loss of static pressure suction that is followed by an increase in the rms of pressure. Breakdown develops asymmetrically. The low-velocity region penetrates the core from the wing. The deployment of an apex flap in a drooping position proved to delay the appearance of breakdown over the wing to an angle of attack of about 8 deg beyond the corresponding value of the unmodified fixed wing. The most efficient drooping angle for the apex flap was found to be 15 deg. The same configuration appears to be equally efficient in controlling breakdown during pitch-up maneuvers. This basic design may prove to be a practical mechanism for the control of aircraft at very high angles of attack. In that case, the concept of the apex flap could be evidenced as a modified LEX or canard.

Acknowledgments

This work was supported by the Air Force Office of Scientific Research, Project AFOSR-91-0310, and was monitored by Daniel Fant.

References

[1]Lee, M., and Ho, C.-M., "Lift Force of Delta Wings," *Applied Mechanics Review*, Vol. 43, 1990, pp. 209–221.

[2]Wood, N. J., and Roberts, L., "The Control of Vortical Lift on Delta Wings by Tangential Leading-Edge Blowing," AIAA Paper 87-0158, Jan. 1987.

[3]Wood, N. J., Roberts, L., and Lee, K. T., "The Control of Vortical Flow on a Delta Wing at High Angles of Attack," AIAA Paper 87-2278, 1987.

[4]Gad-el-Hak, M., and Ho, C.-M., "Unsteady Vortical Flow Around Three-Dimensional Lifting Surfaces," *AIAA Journal*, Vol. 24, No. 5, 1986, pp. 713–721.

[5]Wisser, K., Iwanski, K. T., Nelson, R. C., and Ng, T. T., "Control of Leading-Edge Vortex Breakdown by Blowing," AIAA Paper 88-0504, 1988.

[6]Magness, C., Robinson, O., and Rockwell, D., "Control of Leading-Edge Vortices on a Delta Wing," AIAA Paper 89-0999, 1989.

[7]Magness, C., Robinson, O., and Rockwell, D., "Control of Leading-Edge Vortices on a Delta Wing," NASA/AFOSR/ARO Workshop on Physics of Forced Separation, April 1990.

[8]Gu, W., Robinson, O., and Rockwell, D., "Control of Vortices on a Delta Wing by Leading-Edge Injection," *AIAA Journal*, Vol. 31, No. 7, 1993, pp. 1177–1186.

[9]Lamar, J. E., "Nonlinear Lift Control at High Speed and High Angle of Attack Using Vortex Flow Technology," AGARD-R-740 Special Course on Fundamentals of Fighter Aircraft Design, 1986.

[10]Rao, D. M., and Campbell, J. F., "Vortical Flow Management Techniques," *Progress in Aerospace Sciences*, Vol. 24, 1987, pp. 173–224.

[11]Rediniotis, O. K., Hoang, N. T., and Telionis, D. P., "Multi-Sensor Investigations of Delta Wing High-Alpha Aerodynamics," AIAA Paper 91-0735, Jan. 1991.

[12]Schaeffler, N. W., Hoang, N. T., and Telionis, D. P., "Controlling of Delta Wing Vortices with Vortex Cavity Flaps," 1993 American Society of Mechanical Engineers, Winter Annual Meeting, Paper 93-WAM/NCA-27, 1993.

[13]Klute, S. M., Rediniotis, O. K., and Telionis, D. P., "Flow Control over Delta Wings at High Angles of Attack," AIAA Paper 93-3494, Aug. 1993.

[14]Srinivas, S., Gursul, I., and Batta, G., "Active Control of Vortex Breakdown over Delta Wings," AIAA Paper 94-2215, June 1994.

[15]Gursul, I., Yang, H., and Deng, Q., "Control of Vortex Breakdown with Leading Edge Devices," AIAA Paper 95-06761, Jan. 1995.

[16]Rediniotis, O. K., Hoang, N. T., and Telionis, D. P., "Multi-Sensor Investigation of Delta Wing High-Alpha Aerodynamics," AIAA Paper 91-0735, Jan. 1991.

[17]Rediniotis, O. K., Klute, S. M., Hoang, N. T., and Telionis, D. P., "Pitch-Up Motions of Delta Wings," *AIAA Journal*, Vol. 32, No. 4, 1994, pp. 716–725.

[18]Hoang, N. T., Rediniotis, O. K., and Telionis, D. P., "The Temporal Evolution of a Pair of Streamwise Vortices," *Experiments in Fluids* (to be published).

[19]Wilder, M. C., "Airfoil-Vortex Interaction and the Wake of Oscillating Airfoil," Ph.D. Dissertation, Virginia Polytechnic Inst. and State Univ., Blacksburg, VA, Feb. 1992.

[20]Thompson, S. A., Batill, S. M., and Nelson, R. C., "Delta Wing Surface Pressures for High Angle of Attack Maneuvers," AIAA Paper 90-2813, Aug. 1990.

[21]Atta, R., and Rockwell, D., "Leading Edge Vortices Due to Low Reynolds Number Flow Past a Pitching Delta Wing," *AIAA Journal*, Vol. 28, No. 6, 1990, pp. 995–1004.

[22]Magness, C., Robinson, O., and Rockwell, D., "Unsteady Crossflow on a Delta Wing Using Particle Image Velocimetry," *Journal of Aircraft*, Vol. 29, No. 4, 1992, pp. 707–709.

[23]Magness, C., Robinson, O., and Rockwell, D., "Instantaneous Topology of the Unsteady Leading-Edge Vortex at High Angle of Attack," *AIAA Journal*, Vol. 31, No. 8, 1993, pp. 1384–1391.

[24]Magness, C., Robinson, O., and Rockwell, D., "Laser-Scanning Particle Image Velocimetry Applied to a Delta Wing in Transient Maneuver," *Experiments in Fluids*, Vol. 15, No. 3, 1993, pp. 159–167.

[25]Kegelman, J. T., and Roos, F. W., "Effects of Leading-Edge Shape and Vortex Burst on the Flowfield of a 70-Degree-Sweep Delta Wing," AIAA Paper 89-0086, Jan. 1989.